Elastic scattering of alpha particles

Author: Daniel Hervàs Amargós
Facultat de Física, Universitat de Barcelona, Diagonal 645, 08028 Barcelona, Spain.

Advisor: Xavier Vinyes

Abstract: Elastic scattering of alpha particles is studied at different energies and by different nucleus as targets, using a classical description and the optical model. The results and the different parameters obtained are analysed and compared.

I. INTRODUCTION

Nuclear reactions with alpha particles have been so studied because of their interest in different fields of nuclear physics, since the celebrated Rutherford's experiment. There are several ways to classify reactions according to the collision energies at which they occur, the size of the target or the type of interaction. This work will be about alpha particle collisions with heavier nuclei at different energies and will focus on elastic scattering.

Elastic scattering is the main reaction channel for particle collisions at all incident energies and is therefore a useful experimental tool for the study of nuclear structure and the potential for nucleus-nucleus interaction.

To study the elastic scattering of alpha particles, a classical and a quantum description will be used.

The classical theory even today is useful for describe nuclear collisions, especially for heavy particles with very short wavelengths, since there are large amounts of angular momentum involved in the collision.

To obtain the results, we have used Fortran programs [1] that generate trajectories of a system of classical particles moving under the action of external forces and their mutual interactions, besides several parameters, such as angular momentum, deflection and grazing angle, distance of closet approach or reaction cross section.

Classically the interaction between the two particles is given by a potential with the form:

$$V_{eff} = V_C(r) + \frac{V_0}{1 + \exp\left(\frac{r - R_o}{a}\right)} + \frac{\hbar^2 L^2}{2\mu r^2} \quad , \qquad (1)$$

where $V_C(r)$ is the Coulomb potential of a uniformly charged sphere, defined as

$$V_C = \frac{Z_1 Z_2 e^2}{r} \qquad r \geq R_C \quad ,$$
$$V_C = \frac{Z_1 Z_2 e^2}{2 R_C}\left(3 - \frac{r^2}{R_C^2}\right) \quad r \leq R_C \quad , \qquad (2)$$

with the Coulomb radius R_C.

The second term of Eq. (1) is the nuclear potential and the third is the centrifugal part, which μ the projectile-target reduced mass.

At energies below the Coulomb barrier the particles only interact through their Coulomb fields. At higher energies than the barrier they will begin to be affected by the nuclear interaction, represented here by a Woods-Saxon form factor with adjustable parameters, which are the depth (V_0), the nuclear radius (R_0) and the surface diffuseness (a) of nuclear potential. At much higher energies the nuclear interaction clearly dominates. [2]

The differential cross section obtained with the classical description do not correspond completely with the theory because inelastic interactions remove particles of the elastic channel, furthermore, one should not forget the quantum or wave effects as the interference and the diffraction. [3]

In the quantum description, based on the optical model, these problems can be solved by a complex nuclear potential, since the imaginary part of the potential absorbs flux of the inelastic channel.

The results of the optical model have been obtained by a Fortran program [4] that generates the angular distribution or the ratio between differential cross sections to Rutherford cross sections of the elastic scattering of α-particles.

II. CLASSICAL DESCRIPTION OF ELASTIC SCATTERING

We consider a uniform beam of particles upon a centre of force. As the particle approaches the centre of the force its orbit will deviate from the incident trajectory.

The differential cross section is defined as the number of particles scattered into solid angle (dΩ) per unit time divided by incident intensity. With central forces the element of solid angle is $d\Omega = 2\pi \sin\theta \, d\theta$, where θ is the angle between the scattered and the incident direction.

For any given particle the constants of the orbit are determined by its energy and angular momentum, which we can express in terms of the impact parameter (b) as $L = Mvb$.

The number of particles scattered into dΩ lying between θ and $\theta + d\theta$ must be equal to the number of the incident particles with impact parameter between b and $b + db$. So

$$\frac{d\sigma}{d\Omega} = \frac{b}{\sin\theta}\left|\frac{db}{d\theta}\right| = \frac{L}{M^2 v^2 \sin\theta}\left|\frac{dL}{d\theta}\right| \quad . \qquad (3)$$

We know that the trajectory of the particle in a central force field is symmetric with respect to a line passing through the point of closet approach to the centre of forces (r_0). Therefore, if we call ϕ to the angle between the direction of the incoming asymptote and the closet approach direction, we have a fairly simple relation to the deflection angle (φ), which is the polar angle of the asymptote of the outgoing trajectory.

This relation is [5]

$$\varphi = \pi - 2\phi \quad . \tag{4}$$

Angular momentum and energy are conserved during an elastic collision. So

$$L = M r^2 \frac{d\phi}{dt} \quad , \tag{5}$$

$$E = \frac{1}{2} M \left[\left(\frac{dr}{dt} \right)^2 + r^2 \left(\frac{d\phi}{dt} \right)^2 \right] + V(r) \quad , \tag{6}$$

with V(r) the potential energy of the projectile. Removing dt from both expressions results in the equation of the orbit

$$d\phi = \pm \frac{L/r^2}{\sqrt{2M(E - V(r)) - L^2/r^2}} dr \quad , \tag{7}$$

where the sign is + where the particle approaches the scattering centre and – when has passed the point of closet approach.

Integrating (7) between infinite and r_0 and using (4) we obtain an equation that allows us to calculate the deflection angle φ in terms of the angular momentum if we consider only Coulomb interaction and replace V(r) by the Coulomb potential. This angular momentum as a function of deflection angle, $L(\varphi)$, with Eq. (3) gives us the formula of the differential cross section that Rutherford deduced in 1911:

$$\frac{d\sigma}{d\Omega} = \left(\frac{Z_1 Z_2 e^2}{4E} \right)^2 \frac{1}{\sin^4(\theta/2)} \quad , \tag{8}$$

which is independent of the sign of the charges so the result is the same for both repulsive and attractive fields. We obtain an identical result from quantum mechanics in the non-relativistic limit.

We should distinguish between the deflection angle φ and the scattering angle θ observed in the experiments, which varies between 0 and π. We know that deflection angle can be negative or greater than 2π. For a given φ, the scattering angle θ is determined from the relation $\theta = \pm \varphi - 2n\pi$ with n an integer whose value makes θ lies between 0 and π.

In Rutherford scattering, $L(\varphi)$ is a smooth monotonic function that decreases from π to 0. But with an attractive potential, as nuclear interaction, there can exist two or more values of L that can give rise to the same deflection angle. Then the differential cross section is the sum of contributions from various branches of that function $L(\varphi)$, for which we cannot obtain an analytical solution and need to use numerical methods. [3]

With the introduction of the nuclear field the trajectories are also modified. At large angular momentum the scattering is Coulombic. As L is reduced, near the closet approach, the attractive nuclear field begins to act and starts to modify the orbits, the so-called grazing orbits. One of these grazing trajectories can be an orbiting orbit, which happens when the turning point reach a radius where the nuclear force balance with the Coulomb and centrifugal forces. In this case there is neither velocity nor acceleration and the system continues orbiting. This can only occur for energies below some critical value E_{crit}, which depends upon the deep of the nuclear potential.

For smaller L, the nuclear attraction overcome the repulsive forces and the orbit plunges into the potential well and then emerge with negative deflection angles. [6]

III. OPTICAL MODEL

The aim of the optical model is to be able to remove particles from the elastic channel due to inelastic processes and non-elastic compound nucleus reactions that have an important effect on the cross section.

Since a real potential is not enough, the optical potential has an imaginary part, which takes into account the absorption of the reaction flux from the elastic channel to the non-elastic channels. This is analogous to the scattering and absorption of light by a medium of complex refractive index, this is why it is called the optical model. [7]

The optical potential can be written as

$$V(r) = V_C(r) + V_N(r) + iW_N(r) \quad , \tag{9}$$

where $V_C(r)$ is the Coulomb potential of a uniformly charged sphere, as in Eq. (2), $V_N(r)$ is the real part of the nuclear potential and $W_N(r)$ is the imaginary part, both of which may have a Woods-Saxon form factor like the second term in Eq. (1).

When the optical potential is known, the differential cross section for elastic scattering can be calculated by solving the Schrödinger equation

$$\nabla^2 \psi + \frac{2M}{\hbar^2} (E + V(r) + iW(r)) \psi = 0 \tag{10}$$

using the scattering quantum mechanics theory of partial waves.

The scatter wave function is

$$\psi = -\frac{1}{2ikr} \sum_L (2L+1) P_L(\cos\theta) (e^{2i\delta_L} e^{ikr} - e^{-ikr}) \quad , \tag{11}$$

where k is the wave number, expressed as $k = \sqrt{2ME}/\hbar$, P_L the Legendre polynomial of L^{th} degree and δ_L the phase shifts.

So the differential cross section is given by

$$\frac{d\sigma}{d\Omega} = |\psi|^2 = \frac{1}{4k^2} \left| \sum_L (2L+1) P_L(\cos\theta) (1 - e^{2i\delta_L}) \right|^2 , \tag{12}$$

which integrated for all angles gives the total elastic cross section.

The total cross section is the sum of the shape elastic and the reaction cross section. This last can be obtained summing all the reactions that can occur. [8]

IV. RESULTS AND ANALYSIS

The following results have been obtained using the Fortran programs *"traj_hi1.f"*, *"traj_hi2.f"* and *"traj_hi3.f"*, which are based on a classical description, and the program *"nvgoptalf.f"*, which uses the optical model.

The targets ^{12}C, ^{58}Ni and ^{202}Pb have been analysed for different energies of the incident alpha particles between values near the Coulomb barrier, both above and below, to higher values than E_{crit}.

The adjustable parameters used as the depth of the nuclear potential, the surface diffuseness or the nuclear radius, both the real and the imaginary part, have been obtained from the literature [9] [10]. After analysing different potentials in the first section of the results, the same parameters have been used for obtaining all the others results. [11]

A. Effective Potential and Turning Point

We have previously seen that the effective potential has a repulsive part (Coulomb and centrifugal) and an attractive one (nuclear) and that the classical theory tells us that from a certain distance the nuclear interaction starts to be effective.

In Fig. (1) we plot the distance of closet approach of the α-particle by ^{58}Ni as a function of the angular momentum using four different depth of the nuclear potential. As we can see, there is a jump in the turning point that occurs at the same L value for each of the potentials. This value is approximately $L = 18\ \hbar$ and corresponds to the dashed line.

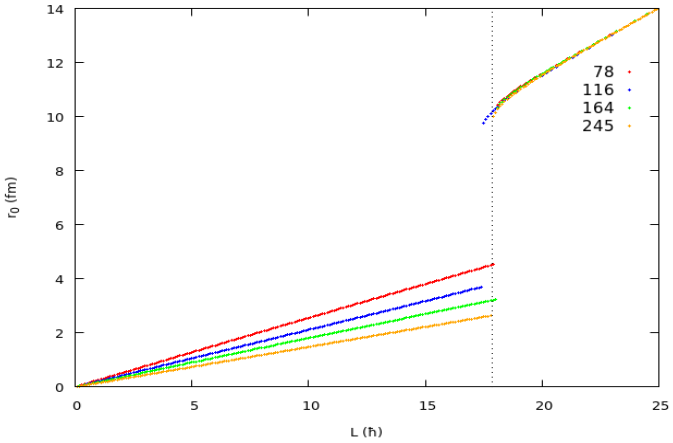

FIG. 1: ^{58}Ni distance of closet approach as a function of L value for the different potentials listed in Table I at 25 MeV.

The effective potential for this value of angular momentum ($L = 18\ \hbar$) is shown in Fig. (2) for the four potentials and we can observe that all of them have the same turning point (where $V_{eff} = E_{C.M.}$).

Different values of the depth of potential give rise to the same result. This is the so-called discrete ambiguity and does not happen to any target at any energy.

In Fig. (3) we see again V_{eff} as a function of r, but this time only for the potential V_0 = 164,7 MeV and for different values of angular momentum.

At small values of L the attractive nuclear potential introduces a dip in the effective potential and for that reason the results obtained in Fig. (1) and Fig. (2) are produced. However the dip disappears at high energies and there is an energy (E_{crit}) from which these results are no longer reproduced and the discrete ambiguity does not appear..

For a given real potential this characteristic energy is [9]

$$E_{crit} = max\left[V(r) + \frac{r}{2}\left(\frac{dV(r)}{dr}\right)\right], \qquad (13)$$

which depends on the depth of the potential and the radius of the target, so if two nuclei have the same real nuclear potential, E_{crit} will be larger for the nucleus with the larger radius (larger mass number A) as is demonstrated in Table I.

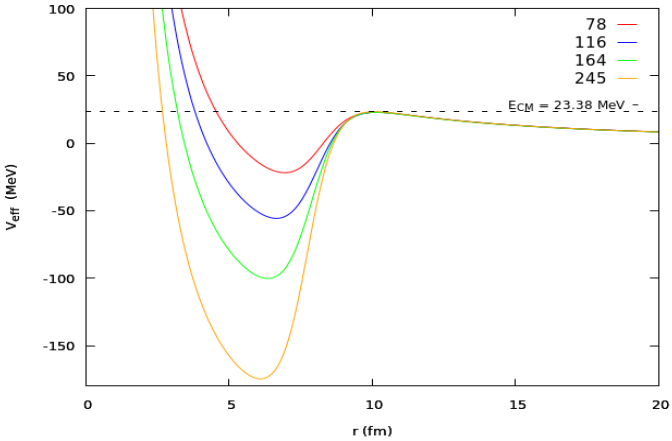

FIG 2: ^{58}Ni effective potentials for L = 18 ħ for the different potentials listed in Table 1. The dashed line corresponds to the energy of the centre of mass of the incident α-particle.

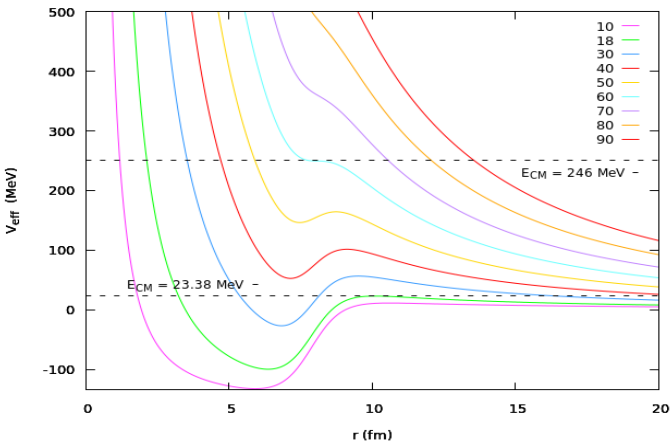

FIG. 3: ^{58}Ni effective potentials for different L values for V_0 = 164,7 MeV. The dashed lines corresponds to the $E_{C.M.}$ of the incident α-particle, the one above is the E_{crit} for this potential.

Target	V_0 (MeV)	E_{crit} (MeV)	B_C (MeV)
^{12}C	116,4	109,3	1,71
	164,7	157,1	1,73
^{58}Ni	78,5	113,5	6,82
	116,4	172,2	6,86
	164,7	246,3	6,94
	245,0	373,2	6,98
^{202}Pb	116,4	229,4	18,23
	164,7	321,5	18,30

TABLE I: Critical energy (E_{crit}) and Coulomb barrier (B_C) for the different depth of the potentials (V_0) of the three targets.

Fig. (4) shows the turning point as a function of L at five different energies for the same value of depth (V_0 = 164,7 MeV) and same target (^{58}Ni).

The Coulomb barrier has a value in this case of B_C = 6,94 MeV.

At 5 MeV, an energy below the Coulomb barrier, the α-particle only interacts through its Coulomb field, as we can expect.

Once the B_C has been overcome, at energies of 10, 25 and 75 MeV, there is a discontinuity in r_0, which corresponds to the angular momentum of the grazing trajectories, which we call L_{gr}, and one of these can be an orbiting orbit as we shall see below.

Above L_{gr} there is only Coulomb interaction basically and below this value is where the nuclear interaction begins to act. L_{gr} increases as the energy increases.

The last energy of Fig. (4) (300 MeV) is above E_{crit}. The discontinuity no longer appears, so there will be no value of L that will result in an orbiting trajectory.

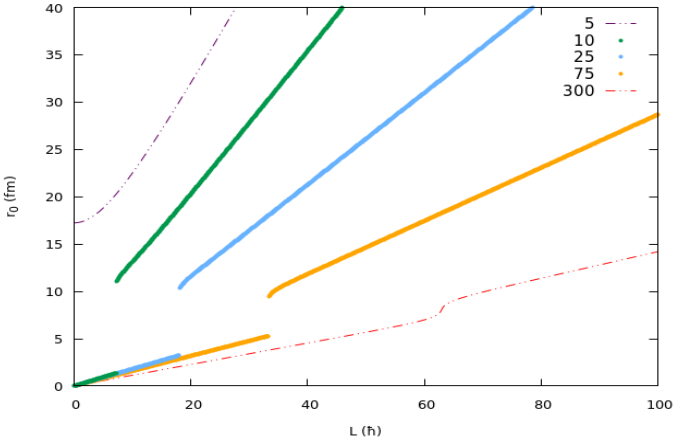

FIG. 4: ^{58}Ni distance of closet approach as a function of L at 5 different energies (in MeV) for V_0 = 164,7 MeV. The dashed lines corresponds to the energies where there is no discontinuity.

B. Trajectories

Fig. (5) shows a set of different types of trajectories of the elastic scattering of 10 Mev α-particles by ^{58}Ni for a set of angular momentums close to the L_{gr} obtained in the previous section with a value of L_{gr} = 7,216 ħ.

We can observe an orbiting orbit for the exact value of L_{gr}, the black colour line. We also see that for a very small variation of this value this phenomenon no longer occurs. For L immediately higher than L_{gr} there are still some grazing trajectories. For still higher L, there are Rutherford trajectories only affected by Coulomb interaction. Finally, for L lower than L_{gr} the nuclear attraction makes that the orbits plunge and emerge on the other side with negative deflection angles.

Such kind of trajectories only will happen at energies between the Coulomb barrier and the critical energy of each target.

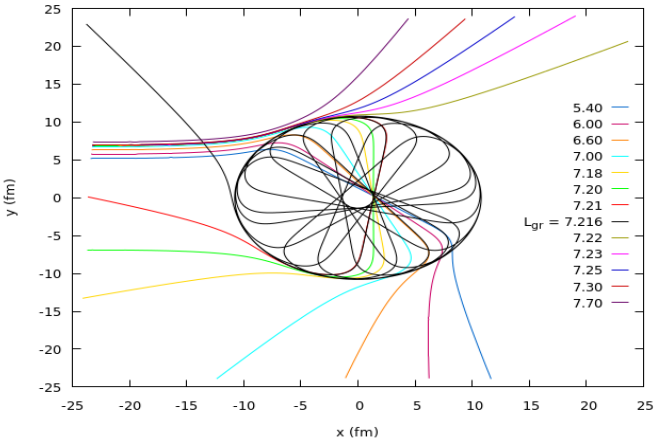

FIG. 5: Alpha particles trajectories when interact with a nucleus of ^{58}Ni at 10 MeV for different values of angular momentum near L_{gr}.

C. Optical Model Predictions

The Fortran code *"nvgoptalf.f"* was developed to calculate the cross sections of elastic scattering reactions at different angles and energies using the optical model [4]. The formula for the strong interaction radius $R = r_0\left(A_1^{1/3} + A_2^{1/3}\right)$ is not expected to hold for the alpha particles, and has been rewritten in the form $R = r_0\, A_2^{1/3}$, being A_2 the target nucleus mass number. [10]

We obtain the differential cross section as ratio to the Rutherford value in terms of the scattering angle by three different targets, Fig. (6). We can see how it varies depending on the energy and the target.

For the same target, as the energy increases the cross section departs from the Rutherford value at smaller angles. Whereas, at the same energy, the cross section departs from Rutherford at smaller angles for smaller atomic number of the target.

The optical model takes into account the presence of quantum or wave effects, which in the classical description are not considered. These effects are manifested as oscillations that occur in the cross sections. They are diffraction patterns that arise as a consequence of the wave nature of the incident particles.

These diffraction patterns depend on the energy incident to the Coulomb barrier.

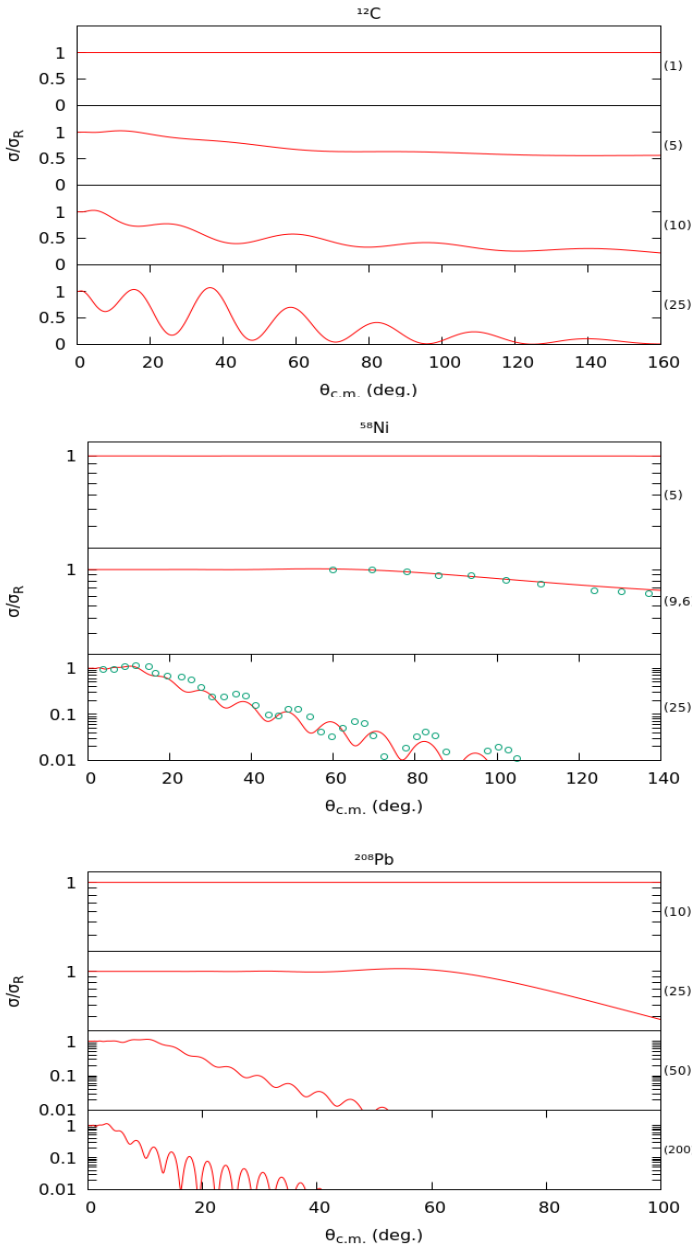

FIG. 6: Comparison of σ/σ_R as a function of the scattering angle θ of the elastic scattering of α-particles on ^{12}C, ^{58}Ni and ^{202}Pb respectively, at different energies (in MeV). The points are the experimental results obtained from [12] in ^{58}Ni at 9,6 MeV and from [13] in ^{58}Ni at 25 MeV.

If E < B_C we can see that the differential cross section is completely the same as the Rutherford and there is no diffraction.

If E > B_C the angular distribution is similar to that given by the Fresnel diffraction formula.

If E >> B_C the oscillations appear and increase at higher energies. The Fraunhofer diffraction type dominates.

V. CONCLUSIONS

As we can see in Fig. (6), in the case of ^{58}Ni, the experimental results of the differential cross section as ratio to the Rutherford cross section are well fitted by the optical model, which implies that this model is a good approximation to describe the elastic scattering of alpha particles by heavy nucleus.

We can also see that there is an important difference in the results depending on the energy incident with respect to the Coulomb barrier, and these differences have also been observed in the results obtained through the classical description.

We know that the classical description does not take quantum effects into account. Due to the short wavelength and the large angular momentum of heavy particles involved, this classical description works well. Taking into account the results obtained, we have been able to prove that even with alpha particles, which are at the limit of the heavy particles, the classical theory provides useful information.

Acknowledgements

I want to thank my advisor Xavier Vinyes for all the advice and help he has given me to do this project and for all his kindness.

[1] F. Salvat and X. Viñas, "traj_hi1.f", "traj_hi2.f" and "traj_hi3.f", Unpublished
[2] Hodgson, Gadioli. *Introductory nuclear physics*, Oxford science publications, 1997. Chapter 23.
[3] F. Salvat. Notes *Elastic collisions of charged particles with atoms*. Chapter 4.
[4] P. E. Hodgson, "nvgoptalf.f", Oxford University Report.
[5] H. Goldstein. *Classical Mechanics* (Addison-Wesley, Reading, MA, 1980)
[6] G. R. Satchler. *Introduction to Nuclear Reactions*. MacMillan, London 1990. pages 132-137
[7] P. E. Hodgson, *The Optical Model of Elastic Scattering*, Clarendon Press, Oxford, 1963.
[8] Hodgson, Gadioli. *Introductory nuclear physics*, Oxford science publications, 1997. Chapter 13.
[9] D. A. Goldberg, S. M. Smith, H. G. Pugh, P. G. Roos, and N. S. Wall, Phys. Rev. C7 1938 (1973)
[10] M. Avrigeanu et al. ArXiv 0808.0566
[11] Parameters: V_0 = 164,7 MeV, R_0 = 1,442 fm, a = 0,52 fm, W = 22,4 MeV, R_W = 1,442 fm, a_W = 0,52 fm, R_C = 1,25 fm.
[12] L. R. Gasques, Phys. Rev. C 67 (2003) 024602; EXFOR-C1165 data file entry.
[13] F. Ballester, E. Casal, J. Díaz, J.B.A England, F. Moriano, J. Phys. G 13 (1987) 1541: EXFOR-01089 data file entry.